Research Article | Vol. 26, No. 24 | 26 Nov 2018 | OPTICS EXPRESS 31363
Optics EXPRESS

Determining the linewidth enhancement factor via optical feedback in quantum dot micropillar lasers

STEFFEN HOLZINGER,[1] SÖREN KREINBERG,[1] BRETT H. HOKR,[2] CHRISTIAN SCHNEIDER,[3] SVEN HÖFLING,[3,4] WENG W. CHOW,[5] XAVIER PORTE,[1,*] AND STEPHAN REITZENSTEIN[1]

[1]*Institut für Festkörperphysik, Quantum Devices Group, Technische Universität Berlin, Hardenbergstraße 36, 10623 Berlin, Germany*
[2]*U.S. Army Space and Missile Defense Command, Huntsville, USA*
[3]*Technische Physik, Universität Würzburg, Am Hubland, 97074 Würzburg, Germany*
[4]*SUPA, School of Physics and Astronomy, University of St Andrews, St Andrews, KY16 9SS, UK*
[5]*Sandia National Laboratories, Albuquerque, NM 87185-1086, USA*
[*]*javier.porte@tu-berlin.de*

Abstract: The linewidth enhancement factor α is a key parameter determining the spectral and dynamical behavior of semiconductor lasers. Here, we propose and demonstrate a method for determining this parameter based on a direct measurement of variations in the laser gain and emission spectrum when subject to delayed optical feedback. We then use our approach to determine the pump current dependent linewidth enhancement factor of a high-β quantum dot micropillar laser. The validity of our approach is confirmed comparing it to two conventional methods, one based on the comparison of the linewidths above and below threshold and the other based on injection locking properties. Furthermore, the pump power dependence of α is quantitatively described by simulations based on a quantum-optical model.

1. Introduction

The emission linewidth and the carrier dynamics are two fundamental characteristics of lasers. In semiconductor lasers, the emission linewidth is enhanced due to the coupling of refractive index and gain to the carrier density [1, 2]. The main parameter describing this effect is the linewidth enhancement or Henry factor (here α-factor), which is known to play a crucial role not only for the spectral characteristics of the laser, but also for its dynamical response and in the sensitivity to optical injection and feedback [3]. Therefore, a number of techniques have been proposed to determine the α-factor in semiconductor lasers. These techniques can be coarsely classified in those that are based on CW spectral measurements [4–8] and the ones that rely on the modulation of some external parameter such as the pump current [9–13]. A comprehensive comparison between several different methods can be found in [14].

Some of the existing methods for determining α depend on particular characteristics of the studied devices. Furthermore, conventional methods usually give only a single scalar value as outcome for α, not being able to track its dependence on key laser parameters like the pump current. These are important limitations for the generic application of those methods, given the fact that α depends on the device characteristics [15] and on its operating conditions [16–18].

In this article we introduce an advanced method for determining the α-factor based on the changes of frequency and gain induced by delayed optical feedback. This technique benefits from the measurement of the gain medium emission from a direction perpendicular to the laser emission direction, so it is particularly well-suited for vertically emitting lasers. It even allows us to characterize for first time the behavior of α in high-β nano- and microlasers, which have received enormous scientific interest and allowed researchers to explore the limits of ultra-small

#340963 https://doi.org/10.1364/OE.26.031363
Journal © 2018 Received 27 Jul 2018; revised 17 Oct 2018; accepted 22 Oct 2018; published 14 Nov 2018

Optics EXPRESS

semiconductor lasers in recent years. There exist already several methods to extract the α-factor using optical feedback that have been successfully applied in e.g. quantum cascade lasers [19]. There, the authors propose measuring the feedback-induced wavelength shift to access the α-factor [20]. However, this method is limited to Fabry-Perot devices subject to low feedback ratios [21]. Other feedback methods based on, e.g. self-mixing interferometry [22], rely on coherent feedback effects which can lead to very short cavities in nanolasers [23]. The method is presented in Sec. 2 and we exemplary apply it to study α in high-β quantum dot (QD) micropillar lasers, an interesting type of microlasers that can for instance be used as coherent drive in quantum nanophotonics [24]. The robustness of our approach is then tested by comparing its outcome with two other well-established methods. In addition, by using the presented method we have found that α in our QD microlasers is not constant but varies with pump current. In order to confirm that finding, in Sec. 3 we have juxtaposed our experimental method with the outcome of a quantum optical model, showing very good quantitative agreement that supports the experimentally determined pump current dependence of the α-factor. The conclusions and outlook of our work are discussed in Sec. 4.

2. Experimental method and determination of α in microlasers

The experiments have been performed with an electrically driven single-mode QD micropillar laser with a diameter of 5 µm. In that device, the gain medium is constituted by a single layer of $In_{0.3}Ga_{0.7}As$ QDs with an area density of $5 \cdot 10^9/cm^2$ in the center of a one-λ GaAs cavity. Highly reflective distributed Bragg reflectors (DBR) made from alternating layers of AlAs and GaAs (27 pairs in the lower and 23 pairs in the upper DBR) form a planar cavity with a quality factor of $Q \simeq 20000$. Precise cleaving of the sample allows for the detection of lateral emission in addition to detection in axial direction as the micropillar is located at the edge of the sample [25]. For further details on the fabrication process of electrically contacted micropillar lasers we refer to [26].

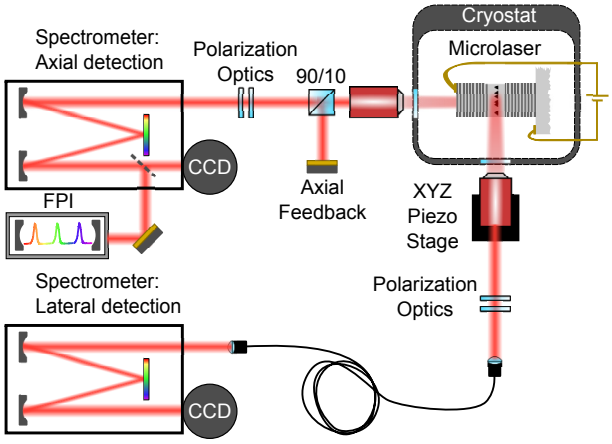

Fig. 1. Sketch of the experimental setup. The QD-micropillar laser is mounted inside a He-flow cryostat and is stabilized at a temperature of $T = 32.00 \pm 0.01$ K. Optical feedback is applied to its axial emission. The spectral properties are measured with charge-coupled devices (CCD) in both the axial and lateral directions. High-resolution spectra are acquired with a Fabry-Perot interferometer (FPI) in the axial direction.

Our micro-electroluminiscence (µEL) setup allows us to simultaneously capture the micropillars' axial and lateral emissions as shown in Fig. 1. The luminescence in both directions is collected by microscope objectives with NA $\sim$ 0.4. The lateral emission is then coupled to a

Optics EXPRESS

single-mode fiber that acts as spatial filter. The optical spectra in both directions are filtered and recorded with two independent spectrometers and CCDs with 42 THz spectral range and 50 GHz resolution. Additionally, a custom-made scanning Fabry-Perot interferometer (7.5 GHz free spectral range, 100 MHz resolution) is used in axial detection for a precise measurement of the spectral position of the fundamental mode.

The alpha factor is defined as [2, 27]

$$\alpha = \frac{\Delta n'}{\Delta n''} = 4\pi \frac{\Delta \nu}{\Delta G}\,, \tag{1}$$

where $\Delta n'$ and $\Delta n''$ denote changes in the real and imaginary parts of the refractive index, respectively. This can be rewritten as a function of observables in our experiment, namely the optical frequency shift of the fundamental mode $\Delta\nu$ and the change in modal gain ΔG.

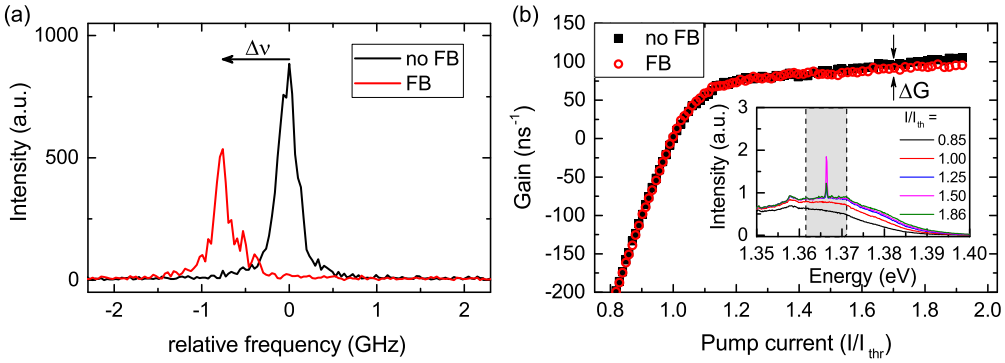

Fig. 2. (a) Exemplary high-resolution emission spectra of a QD micropillar showing the feedback-induced shift of the lasing mode at $I = 1.9\, I_{th}$. (b) Extracted modal gain as a function of the pump current with and without optical feedback (FB). The inset depicts spectra of the QD emission measured in lateral detection. The shaded gray area represents the integration range of the gain contributing to the lasing mode.

Delayed optical feedback (in the axial direction) modifies the laser losses and causes a change in its gain and spectrum. We exploit this effect to get insight into the α-factor of the QD micropillar laser. We first measure the feedback-induced frequency shift of the fundamental mode with the FPI as can be seen in Fig. 2(a). Here we compare the scenario in absence of feedback with the case of maximum feedback strength. The loss channels in the external cavity are the 90/10 beam splitter, the microscope objective, the external cavity mirror and the top DBR mirrors, resulting in about 40% of the light being coupled back onto the microlaser facet, from which about 10% finally reaches the active medium. This result is consistent with previous numerical simulations on this feedback-coupled system [28]. To avoid alignment losses, a piezo-tuning mirror has been used to align the feedback spot onto the microlaser facet with below 0.4 µm precision.

We want to highlight that the feedback parameters must be chosen such that we work in a feedback regime that preserves narrow spectral lines [29] as it is otherwise impossible to define a precise shift of the wavelength. In our case we choose an external cavity length of 1.58 m which is greater than the maximum coherence length of the microlaser (~40 cm). Our approach thus does not need coherent feedback as in the case of self-mixing interferometry which is beneficial when applying it to nanolasers. Hayenga et al. for example report on metallic nanolasers with a minimum linewidth of ~0.7 nm at an emission wavelength of 1300 nm resulting in a coherence length 0.8 mm [23]. Thus, being able to work in the regime of incoherent feedback is convenient at cryogenic temperatures where a feedback mirror would be technologically challenging to implement.

Optics EXPRESS

The corresponding change in modal gain can be extracted from the lateral spectra as recorded with the spectrometer. We do so by integrating the measured QD-gain intensity around the actual lasing mode (see inset of Fig. 2(b)). Lasing emission is directed towards axial detection but there is also a significant amount of scattered light from the sidewalls of microlaser. Thus, we always need to subtract the scattered light of the mode from the integral, which is done by comparing both spectra from axial and lateral detection. Here it is vital that a linear polarizer is used in both detection paths to record only the emission that is related to the QD gain corresponding to respective lasing mode. This way we can choose an area of the axial spectrum that corresponds to the QD gain feeding the lasing mode. Noteworthy, we choose spectrally the minimum integration range from the lateral spectrum that still shows a clear kink in the gain curve leading to clear carrier clamping. Smaller ranges show a very shallow kink (not enough gain integrated) and for larger ranges the gain above threshold is not totally clamped due to excess of amplified spontaneous emission. The further the gain is spectrally detuned from the lasing mode, the less efficient is the coupling between both. Thus, the QDs with these spectral properties do not strongly contribute to the mode via stimulated emission and hence mainly radiate spontaneously. This however, may lead to gain compression of the lasing mode because the injected carriers may recombine in the spectrally and spatially far-off gain regions, before they can fill the spectral or spatial hole burned by the lasing mode. For a correct scaling of the modal gain we introduce the assumptions from [30] that the modal gain is zero at inversion and that the maximum modal gain is clamped to the cavity loss rate κ with

$$\kappa = \frac{2\pi\nu_0}{Q} = 105.62\,\mathrm{ns}^{-1}\,, \tag{2}$$

where ν_0 denotes the frequency of the fundamental mode.

As it is shown in Fig. 2(b), optical feedback reduces the effective cavity loss rate of the coupled cavity ($\kappa_{eff} < \kappa$) and thus the maximal modal gain. Averaging the feedback-induced mode shift and modal gain reduction along the input-output curve, we can calculate a first approximation to α with our method, which is $\alpha_{FB} = 2.3 \pm 0.3$. However, this quantity ignores any dependence with pump current, as we will discuss later in this article.

Comparison to other methods of determining α

To prove the validity of the above presented method we compare the result to well-established schemes for determining α. First, we apply an approach based on the Schawlow-Townes law for the linewidth dependence with the output power [31]. Following the derivation in [5], the linewidth of the fundamental mode $\Delta\nu$ is a function of the inverse optical output power P:

$$\Delta\nu = \Delta\nu_0 + \frac{\zeta_{\gtrless}}{P}\,, \tag{3}$$

with $\Delta\nu_0$ depicting the minimal linewidth of the microlaser given by occupation fluctuations. The characteristic slopes of the linewidth below and above threshold are $\zeta_<$ and $\zeta_>$, respectively. The α-factor can then be determined by the following equation:

$$\alpha = \sqrt{2\frac{\zeta_>}{\zeta_<} - 1}\,, \tag{4}$$

as the linewidth above threshold is broadened by $1 + \alpha^2$ while below threshold noise contributions are twice as high than above. Thus, we determine α from the slopes extracted from Fig. 3. The (FWHM) linewidth below threshold is determined from a Voigt fit of the fundamental mode recorded with the CCD while the linewidth above threshold is extracted from a Lorentzian fit of the FPI spectra. Taking into account the instrument response functions of the device used to

Optics EXPRESS

acquire optical spectra one ends up with Voigt lineshapes for the CCD and Lorentzian ones for the FPI, respectively. Thus, the linewidth enhancement factor obtained from the Schawlow-Townes linewidth-power dependencies is $\alpha_{S-T} = 2.4 \pm 0.2$.

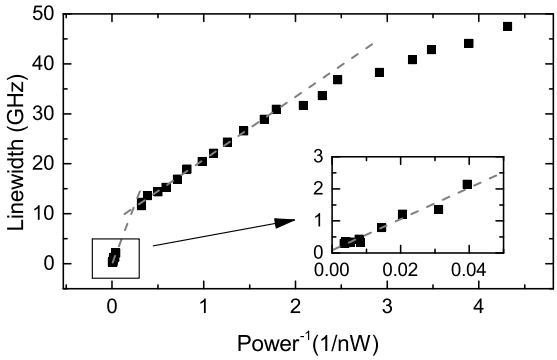

Fig. 3. Emission linewidth plotted as a function of the inverse optical output power (measured with a powermeter). The α-factor can be determined from linear fits (dashed lines) of the linewidths above (see inset) and below threshold.

Another well-established method for determining the α-factor is via the slopes of the injection locking cone. For this experiment a tunable laser (master) is coupled to the optical path where previously the feedback mirror was placed. From a previous study on high-β micropillar lasers [32] we expect partial phase and frequency locking of the micropillar laser (slave) to the master laser. The seminal work of Lang [33] predicts that the locking range of a semiconductor laser is given by the following inequality:

$$CK_{eff}\sqrt{1+\alpha^2} < \nu_{locking} < CK_{eff}\,, \tag{5}$$

where C is a constant related only to device parameters and K_{eff} is the effective injection strength, which does not have to be explicitly known to determine the α-factor. Fig. 4 depicts the normalized intensity of the frequency-locked slave oscillation as a function of the solitary master and slave frequencies detuning Δ for different pump currents, i.e. $I = 1.5\,I_{th}$ in Fig. 4(a) and $I = 1.7\,I_{th}$ in Fig. 4(b). We want to note that in Fig. 4(a), the color-coded intensity at positive detunings is abnormally high outside the injection locking cone, which we attribute to partial locking effects [34]. Nevertheless, this effect appears only at high injection strengths and does not affect our calculations here. The α-factor is calculated from the edges of the locking cone at positive and negative detunings [35]:

$$\alpha = \sqrt{\left(\frac{m_-}{m_+}\right)^2 - 1}\,, \tag{6}$$

with m_- and m_+ being the negative and positive slope of the locking tongue, respectively. For the two measured pump currents we get $\alpha_{IL}^{1.5I_{th}} = 2.3 \pm 0.3$ and $\alpha_{IL}^{1.7I_{th}} = 1.9 \pm 0.3$.

When comparing our proposed method with the two well established techniques for determining the α-factor, we conclude that the former yields a consistent result that is within the error bars of the well-known schemes. In addition, our delayed optical feedback based method naturally gives access to the pump power dependence of α, which is of interest to address particular dynamical behaviors.

Optics EXPRESS

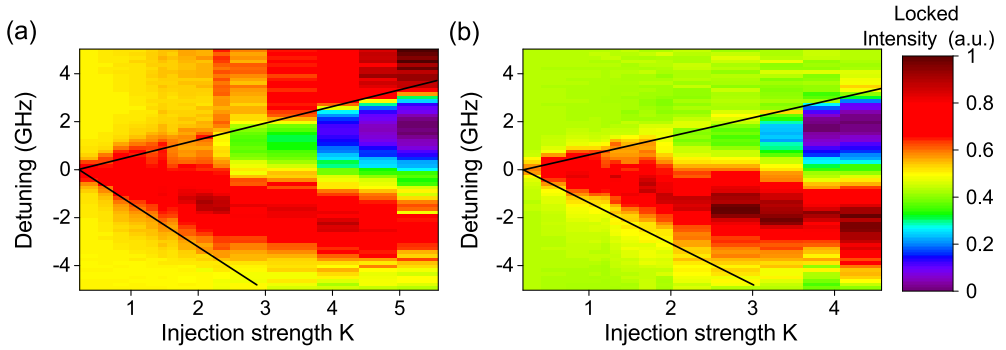

Fig. 4. Determining α from injection locking. Normalized intensity of the frequency-locked oscillation as a function of detuning Δ between the master laser and slave microlaser for different pump currents (a) $I = 1.5\, I_{th}$ and (b) $I = 1.7\, I_{th}$. Solid lines indicate the edge of the locking cones.

3. Quantum optical modeling and pump current dependence of α

Next, we further support our method with numerics based on a quantum-optical model. This model is originally derived in the Heisenberg picture using a cluster expansion method to obtain a closed set of equations of motion for the polarization p, photon population n_p and electron (hole) carrier population $n_e(n_h)$ [36, 37]. The linewidth enhancement factor is determined from calculating the gain and carrier-induced refractive spectra. The amplitude gain $g(\omega)$ and carrier-induced refractive index $\delta n(\omega)$ for a QW layer embedded with QDs are obtained from the interband polarization, $p_{ij}(\omega)$:

$$K\delta n(\omega) + ig(\omega) = -\frac{\omega}{\varepsilon_0 n_{bg} c w E(\omega)} \sum_{i,j} \mu_{ij} p_{ij}(\omega) \tag{7}$$

where i, j are the discrete and continuous labels for QD and QW states respectively, c and ε_0 is the speed of light and permittivity in vacuum, n_{bg} is the background refractive index, K is the laser field wavevector, w width of the QW width embedding a sheet QD density of N_{dot}, $E(\omega)$ is a weak laser probe field at frequency ω, and the summations are over all possible electron-hole QD and QW transitions.

For the polarization we solve the following equation of motion

$$\frac{d}{dt} p_{ij} = i\omega_{ij} p_{ij} + i\Omega_{ij}(1 - n_i^e - n_j^h) + S_{ij}^{c-c} + S_{ij}^{c-p}\,, \tag{8}$$

where ω_{ij} and Ω_{ij} are the renormalized transition and Rabi frequencies , n_i^e and n_j^h are the electron and hole populations in states i and j. Dephasing contributions due to carrier-carrier and carrier-phonon scatterings are described by the complex terms $S_{ij}^{c-c}(\omega)$ and $S_{ij}^{c-p}(\omega)$, respectively. Details for their evaluation are described in the literature [36]. The steady-state solution to Eq. 8 is used in Eq. 7. Inhomogeneous broadening due to sample dimensional or alloy fluctuations, are taken into account with a statistical average over a range of band-gap energy assuming a weighting described by a normal distribution characterized by an inhomogeneous broadening width $\Delta_{inh} \simeq 30$ meV.

Figure 5 summarizes the results of the present work, depicting together as a function of the pump current the values of α acquired with the different experimental methods and with the theory. For comparison, we have added the input-output dependencies with and without feedback are plotted as a reference. Noteworthy, there is a rollover in the input-output curves beyond a

Optics EXPRESS

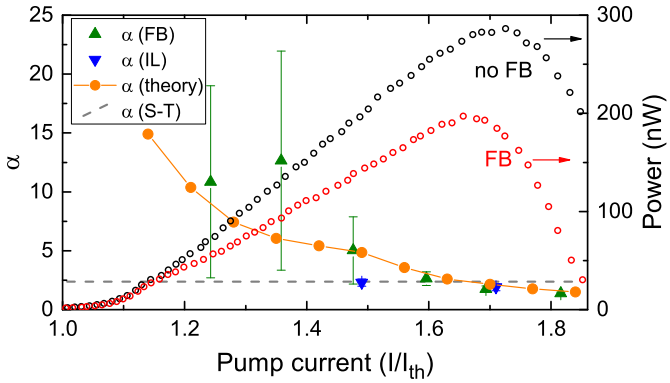

Fig. 5. Pump current dependence of the α-factor. The proposed method (green triangles), theory (orange circles), injection locking (blue triangles) and the Schawlow-Townes-like law (dashed grey line) are compared. The input-output characteristic (right axis, red and black dots for feedback and no-feedback scenarios, respectively) are plotted as references.

certain pump current above threshold, this effect originates when the gain maximum shifts away from the cavity mode. The reduced output power in the presence of feedback can be explained by gain competition with the fundamental mode with orthogonal polarization. For more details on the influence of feedback on the switching dynamics in these microlasers causing this behavior we refer to [28]. Beyond the consistent matching of the different methods, the main message in Fig. 5 is the clear pump current dependence of the α-factor that can be observed in the different methods that are sensitive to this parameter. Here, for our feedback method we do not take the averaged frequency and gain shifts, but we determine them piece-wise along the input output. The error bars are bigger around threshold because the gain change determination is less precise there. Interestingly, we then obtain an α-factor that decreases towards a constant value around ~ 2 for high pump currents, which is accurately reproduced by the parameters-matched model. The model explains the high values of α at low pump currents due to a refractive index decrease caused by frequency pulling towards the quantum well (QW) gain [38]. This occurs in microlasers with low indium content QDs, where the energy levels of the QDs are very close to those of the QW with an electron (hole) distance of 10 meV (19 meV) to the conduction (valence) band edge of the wetting layer. Therefore, the QW is significantly populated even for low pump currents and influences α. Moreover, the detailed model pump-dependence curve unveils two distinct decay constants for α that can be explained taking into account the dominant contributions to the gain at different currents. For low pump currents, the gain is dominated by the QDs. However, around $\sim 1.5 I/I_{th}$ the QW gain starts to dominate, leading to a shallower decay of α.

If we take into account that the linewidth decreases along the input-output curve (cf. Fig. 3), those findings are in good agreement with the dependence between α and linewidth found in [15, 39] for various laser types.

4. Conclusions

To conclude, we have proposed a novel method for determining the linewidth enhancement factor in vertically emitting lasers based on the changes of gain and spectrum when optical feedback is applied. We have applied this method to explore α for the first time for a QD microlaser. The obtained results are in quantitative agreement with the outcome of two other well established methods in literature. Moreover, using our approach we have unveiled a strong pump current dependence of α that is accurately reproduced and explained by numerical modeling from

Optics EXPRESS

quantum optical theory. Noteworthy, our approach is specially well-suited for characterizing the α-factor in high-β nanolasers, in contrast to the other presented methods. For example, the injection locking-based method becomes increasingly imprecise the higher β is. The partial nature of locking in high-β lasers prevents one to precisely determine the locking range as most photons remain in the unlocked solitary nanolaser mode. The amount of injection needed to reach locked oscillation will then rather lead to coherent pumping than locking. In addition, nanolasers often suffer from thermally induced linewidth broadening at high pump powers [40, 41] so that the linewidth method cannot be applied to determine α. Therefore, we believe that our proposed method will become an important tool to determine α and consequently to better understand and tailor the dynamical and spectral properties of nanolasers in the future.

Funding

European Research Council under the European Union's Seventh Framework Program (ERC 615613); German Research Foundation (CRC 787); U.S. Department of Energy (DE-AC04-94AL85000).

Acknowledgments

We are grateful to I. Fischer for helpful comments and discussion. W.W.C. thanks for travel support by the German Research Foundation.

References

1. M. W. Fleming and A. Mooradian, "Fundamental line broadening of single-mode (GaAl)As diode lasers," Appl. Phys. Lett. **38**, 511–513 (1981).
2. C. Henry, "Theory of the linewidth of semiconductor lasers," IEEE J. Quantum Electron. **18**, 259–264 (1982).
3. M. Osinski and J. Buus, "Linewidth broadening factor in semiconductor lasers–an overview," IEEE J. Quantum Electron. **23**, 9–29 (1987).
4. I. D. Henning and J. V. Collins, "Measurements of the semiconductor laser linewidth broadening factor," Electron. Lett. **19**, 927–929 (1983).
5. Z. Toffano, A. Destrez, C. Birocheau, and L. Hassine, "New linewidth enhancement determination method in semiconductor lasers based on spectrum analysis above and below threshold," Electron. Lett. **28**, 9–11 (1992).
6. A. Villafranca, J. A. Lazaro, I. Salinas, and I. Garces, "Measurement of the linewidth enhancement factor in dfb lasers using a high-resolution optical spectrum analyzer," IEEE Photonics Technol. Lett. **17**, 2268–2270 (2005).
7. R. Hui, A. Mecozzi, A. D'Ottavi, and P. Spano, "Novel measurement technique of alpha factor in dfb semiconductor lasers by injection locking," Electron. Lett. **26**, 997–998 (1990).
8. C. Wang, K. Schires, M. Osiński, P. J. Poole, and F. Grillot, "Thermally insensitive determination of the linewidth broadening factor in nanostructured semiconductor lasers using optical injection locking," Sci. Rep. **6**, 27825 (2016).
9. C. Harder, K. Vahala, and A. Yariv, "Measurement of the linewidth enhancement factor α of semiconductor lasers," Appl. Phys. Lett. **42**, 328–330 (1983).
10. M. Osiński, D. Gallagher, and I. White, "Measurement of linewidth broadening factor in gain-switched InGaAsP injection lasers by CHP method," Electron. Lett. **21**, 981–982 (1985).
11. Y. Sorel and J. F. Kerdiles, "Simple measurement of fiber dispersion and of chirp parameter of intensity modulated light emitter," J. Light. Technol. **11**, 1937–1940 (1993).
12. J. Jeong and Y. Park, "Accurate determination of transient chirp parameter in high speed digital lightwave transmitters," Electron. Lett. **33**, 605–606 (1997).
13. A. Consoli, B. Bonilla, J. M. G. Tijero, and I. Esquivias, "Self-validating technique for the measurement of the linewidth enhancement factor in semiconductor lasers," Opt. Express **20**, 4979–4987 (2012).
14. T. Fordell and A. M. Lindberg, "Experiments on the linewidth-enhancement factor of a vertical-cavity surface-emitting laser," IEEE J. Quantum Electron. **43**, 6–15 (2007).
15. G. Giuliani, S. Donati, and W. Elsässer, "Measurement of linewidth enhancement factor of different semiconductor lasers in operating conditions," Proc. SPIE 6184, Semicond. Lasers Laser Dyn. II pp. 61841D–1–61841D–9 (2006).
16. P. P. Vasil'ev, I. H. White, and J. Gowar, "Fast phenomena in semiconductor lasers," Rep. Prog. Phys. **63**, 1997–2042 (2000).
17. B. Lingnau, K. Lüdge, W. W. Chow, and E. Schöll, "Failure of the α factor in describing dynamical instabilities and chaos in quantum-dot lasers," Phys. Rev. E **86**, 065201 (2012).
18. B. Herzog, B. Lingnau, M. Kolarczik, Y. Kaptan, D. Bimberg, A. Maaßdorf, U. W. Pohl, R. Rosales, J.-H. Schulze, A. Strittmatter, M. Weyers, U. Woggon, K. Lüdge, and N. Owschimikow, "Strong amplitude-phase coupling in submonolayer quantum dots," Appl. Phys. Lett. **109**, 201102 (2016).

Optics EXPRESS

19. L. Jumpertz, F. Michel, R. Pawlus, W. Elsässer, K. Schires, M. Carras, and F. Grillot, "Measurements of the linewidth enhancement factor of mid-infrared quantum cascade lasers by different optical feedback techniques," AIP Adv. **6**, 015212 (2016).
20. N. Schunk and K. Petermann, "Numerical analysis of the feedback regimes for a˜single-mode semiconductor laser with external feedback," IEEE J. Quantum Electron. **24**, 1242–1247 (1988).
21. L. Jumpertz, M. Carras, K. Schires, and F. Grillot, "Regimes of external optical feedback in 5.6 μm distributed feedback mid-infrared quantum cascade lasers," Appl. Phys. Lett. **105**, 131112 (2014).
22. Y. Yu, G. Giuliani, and S. Donati, "Measurement of the linewidth enhancement factor of semiconductor lasers based on the optical feedback self-mixing effect," IEEE Photonics Technol. Lett. **16**, 990–992 (2004).
23. W. E. Hayenga, H. Garcia-Gracia, H. Hodaei, C. Reimer, R. Morandotti, P. LiKamWa, and M. Khajavikhan, "Second-order coherence properties of metallic nanolasers," Optica **3**, 1187–1193 (2016).
24. S. Kreinberg, T. Grbešić, M. Strauß, A. Carmele, M. Emmerling, C. Schneider, S. Höfling, X. Porte, and S. Reitzenstein, "Quantum-optical spectroscopy of a two-level system using an electrically driven micropillar laser as a resonant excitation source," Light Sci. Appl. **7**, 41 (2018).
25. A. Musiał, C. Hopfmann, T. Heindel, C. Gies, M. Florian, H. A. M. Leymann, A. Foerster, C. Schneider, F. Jahnke, S. Höfling, M. Kamp, and S. Reitzenstein, "Correlations between axial and lateral emission of coupled quantum dot–micropillar cavities," Phys. Rev. B **91**, 205310 (2015).
26. C. Böckler, S. Reitzenstein, C. Kistner, R. Debusmann, A. Löffler, T. Kida, S. Höfling, A. Forchel, L. Grenouillet, J. Claudon, and J. M. Gérard, "Electrically driven high-q quantum dot-micropillar cavities," Appl. Phys. Lett. **92**, 091107 (2008).
27. C. Henry, N. Olsson, and N. Dutta, "Locking range and stability of injection locked 1.54 um ingaasp semiconductor lasers," IEEE J. Quantum Electron. **21**, 1152–1156 (1985).
28. S. Holzinger, C. Redlich, B. Lingnau, M. Schmidt, M. von Helversen, J. Beyer, C. Schneider, M. Kamp, S. Höfling, K. Lüdge, X. Porte, and S. Reitzenstein, "Tailoring the mode-switching dynamics in quantum-dot micropillar lasers via time-delayed optical feedback," Opt. Express **26**, 22457–22470 (2018).
29. R. Tkach and A. Chraplyvy, "Regimes of feedback effects in 1.5-um distributed feedback lasers," J. Light. Technol. **4**, 1655–1661 (1986).
30. G. Björk, A. Karlsson, and Y. Yamamoto, "Definition of a laser threshold," Phys. Rev. A **50**, 1675–1680 (1994).
31. A. L. Schawlow and C. H. Townes, "Infrared and optical masers," Phys. Rev. **112**, 1940–1949 (1958).
32. E. Schlottmann, S. Holzinger, B. Lingnau, K. Lüdge, C. Schneider, M. Kamp, S. Höfling, J. Wolters, and S. Reitzenstein, "Injection locking of quantum-dot microlasers operating in the few-photon regime," Phys. Rev. Appl. **6**, 044023 (2016).
33. R. Lang, "Injection locking properties of a semiconductor laser," IEEE J. Quantum Electron. **18**, 976–983 (1982).
34. Hua Li, T. Lucas, J. McInerney, M. Wright, and R. Morgan, "Injection locking dynamics of vertical cavity semiconductor lasers under conventional and phase conjugate injection," IEEE J. Quantum Electron. **32**, 227–235 (1996).
35. G. Liu, X. Jin, and S. L. Chuang, "Measurement of linewidth enhancement factor of semiconductor lasers using an injection-locking technique," IEEE Photonics Technol. Lett. **13**, 430–432 (2001).
36. W. W. Chow and F. Jahnke, "On the physics of semiconductor quantum dots for applications in lasers and quantum optics," Prog. Quantum Electron. **37**, 109–184 (2013).
37. W. W. Chow, F. Jahnke, and C. Gies, "Emission properties of nanolasers during the transition to lasing," Light. Sci. Appl. **3**, e201 (2014).
38. M. Lorke, F. Jahnke, and W. W. Chow, "Excitation dependences of gain and carrier-induced refractive index change in quantum-dot lasers," Appl. Phys. Lett. **90**, 3–5 (2007).
39. G. Giuliani, S. Donati, and W. Elsässer, "Measurement of linewidth enhancement factor variations in external cavity semiconductor lasers," EQEC '05. Eur. Quantum Electron. Conf. 2005. **25**, 13 (2005).
40. Y. Gong, B. Ellis, G. Shambat, T. Sarmiento, J. S. Harris, and J. Vuckovic, "Nanobeam photonic crystal cavity quantum dot laser," Opt. Express **18**, 8781–8789 (2010).
41. S. T. Jagsch, N. V. Triviño, F. Lohof, G. Callsen, S. Kalinowski, I. M. Rousseau, R. Barzel, J.-F. Carlin, F. Jahnke, R. Butté, C. Gies, A. Hoffmann, N. Grandjean, and S. Reitzenstein, "A quantum optical study of thresholdless lasing features in high-β nitride nanobeam cavities," Nat. Commun. **9**, 564 (2018).